

Supplementary Information for

Molecular mechanism of abnormally large non-softening deformation in a tough hydrogel

Ya Nan Ye, Kunpeng Cui*, Wei Hong, Xueyu Li, Chengtao Yu, Dominique Hourdet, Tasuku Nakajima, Takayuki Kurokawa and Jian Ping Gong*

* Kunpeng Cui

Email: kpcui@sci.hokudai.ac.jp

* Jian Ping Gong

Email: gong@sci.hokudai.ac.jp

This PDF file includes:

Supplementary text

Table S1

Figures S1 to S9

SI References

Supplementary text

The structure of B gel.

The average distance between adjacent micelles, d , is calculated by(1)

$$d = \frac{2\pi}{q_{peak}} \quad (1)$$

where q_{peak} is the peak position in 1D scattering profile. The number density of end block chain per volume in B gel, v_B , is calculated by

$$v_B = \left(\frac{2w_{PBMA}N_A}{M_{PBMA}} \right) \times \frac{1}{\frac{2w_{PBMA}}{\rho_{PBMA}} + \frac{w_{PMAA}}{\rho_{PMAA}} + \frac{w_w}{\rho_w}} \quad (2)$$

where $2w_{PBMA}$, w_{PMAA} , and w_w are the weight fractions of total end-blocks PBMA, mid-block PMAA, and water in the B gel, respectively. N_A is Avogadro's number, and M_{PBMA} is the number-averaged molecular weight of one end-block in the triblock copolymer. The ρ_{PBMA} , ρ_{PMAA} and ρ_w are the densities of PBMA (1.053 g/cm³), PMAA (1.29 g/cm³), and water (0.997 g/cm³), respectively.

For the triblock copolymer PBMA-b-PMAA-b-PBMA with polymerization degree 93-302-93, $2w_{PBMA}$, w_{PMAA} , w_w and M_{PBMA} are 5.95 wt%, 5.85 wt%, and 88.2 wt%, and 13224 g/mol, respectively. So, the $v_B = 2.75 \times 10^{24} \text{ m}^{-3}$.

The aggregation number, N , or the number of end-blocks per micelle, is calculated by

$$N = v_B \times d^3 \quad (3)$$

Here $d = 34.6 \text{ nm}$, which gives a $N = 114$.

The volume of a micelle v and its radius r is calculated by the following equation:

$$v = \frac{M_{PBMA}}{\rho_{PBMA}N_A} N = \frac{4}{3}\pi r^3 \quad (4)$$

It gives a PBMA micelle radius of $r = 8.3 \text{ nm}$.

The B gel was prepared with a polymer concentration of 0.19 (wt/wt) that the bridge fraction reaches the saturated state according to the previous study(2). The bridge fraction for micelles in glassy state is around 0.6 according to the prediction of dissipative particle dynamics model(3), which gives a number of bridged end-block chains in one micelle of

$$f = N \times 0.6 \quad (5)$$

So, the connectivity $f = 69$.

The numbers of bridged end-block chain per unit volume in B gel:

$$v_{B-eff} = v_B \times 0.6 \quad (6)$$

So, the v_{B-eff} is $= 1.65 \times 10^{24} \text{ m}^{-3}$. The numbers of bridged mid-block chain per unit volume in B gel is $\frac{1}{2}v_{B-eff}$.

The mean-squared end-to-end distance of mid-block PMAA chain in Gaussian conformation is:

$$R_{Guassian} = \sqrt{Nb} \quad (7)$$

where the N and b is the Kuhn number (302) and Kuhn length (0.33 nm) of the PMAA chain, respectively.(4) So $R_{Guassian} = 5.73 \text{ nm}$. The actual end-to-end distance of PMAA equals to $d_0 - 2r = 18 \text{ nm}$. So, the chain in B gel is at pre-stretched state with a stretch ratio λ_{pre} of about 3. According to the rubber elasticity, the Young's modulus of B gel can be estimated(5):

$$E = 3 \frac{v_{B-eff}}{2} k_B T \lambda_{pre}^2 \quad (8)$$

Here k_B is Boltzmann constant ($1.38 \times 10^{23} \text{ J} \cdot \text{K}^{-1}$), T is the experimental temperature (298 K). Equation 8 gives a modulus of 0.09 MPa, which agrees reasonably well with experiment result of 0.04 MPa.

The contour length of one mid-block PMAA chain is calculated with the relation $R_{max} = Nb$, which is 99.7 nm.

Mechanochemical color-changing test

Here we further confirm that the irreversible structure change in glue-B gel is not due to the chain scission of the mid-block. According to the literature, if the chain scission occurs, it generates mechanoradicals, which can be detected by mechanochemical color-changing test. The mechanoradicals can react with water to form hydrogen peroxide, which in turn oxidizes ferrous ions (Fe^{2+}) into ferric ions (Fe^{3+}) in the Fenton reaction (Inset of **FIG. S9a**). The detection limit of this mechanochemical color-changing method is around 10^{-6} mol/L .(6)

First, we calculate the amount of mechanoradicals generated by assuming that the irreversible energy is used for chain scission of mid-block. According to the Lake-Thomas model, the energy required for scissoring one chain is $E_{chain} = NU_b$ where N is the repeated

number of monomer/bond, U_b is the bond energy.(7) To rupture one molar midblock chains needs energy $E_{\text{chain}} \cong 1 \times 10^8 \text{ J} \cdot \text{mol}^{-1}$ by using $N = 302$ and $U_b = 350 \text{ kJ} \cdot \text{mol}^{-1}$.(8) The irreversible energy at $\lambda_{\text{max}} = 4$ is $U_{\text{hys,irev}} \cong 10^6 \text{ J} \cdot \text{m}^{-3}$, The number density of fractured mid-blocks is $n_{\text{fracture}} = U_{\text{hys,irev}}/E_{\text{chain}} \cong 10^{-5} \text{ mol} \cdot \text{L}^{-1}$. Each fracture mid-block generates two mechanoradicals. So, if $\sim 10^{-5} \text{ mol/L}$ mechanoradicals are generated, it can be detected by this method.

We introduced ferrous ions and xylenol orange (XO), an indicator of ferric ions, into the glue-B gel and then stretched the gel to $\lambda = 4$. As shown in **Fig. S9a**, the ultraviolet (UV)-visible light absorption spectrum of stretched sample is the same as that of undeformed sample, and no characteristic peak around 580 nm accounting for the absorption of Fe^{3+} -XO appears, suggesting no or negligible chain scission during stretching. On the other hand, the glue-C gel made from chemically crosslinked PMAA as the first network shows obvious characteristic peak around 580 nm, demonstrating the occurrence of chain scission during stretching (**Fig. S9b**). These results further confirm that the irreversible hysteresis of the glue-B gel is not due to the covalent bond rupture of the PMAA mid-block strands but due to pullout of the end-blocks from micelles.

Tab. S1. Description of triblock copolymers.

Triblock copolymer ^{a)} $A_m B_n A_p$	^{b)} f_B	^{c)} M_n (kg/mol)	^{d)} M_w/M_n
$A_{81} B_{159} A_{60}$	0.53	33.69	1.43
$A_{120} B_{168} A_{112}$	0.42	47.39	1.42
$A_{100} B_{204} A_{96}$	0.51	45.38	1.34
$A_{95} B_{302} A_{95}$	0.61	53.64	1.31
$A_{105} B_{390} A_{105}$	0.65	73.66	1.43

^{a)}The subscripts of m, n and p represent the degree of polymerization of the endblock, midblock and endblock respectively. A and B represent poly(butyl methacrylate) (PBMA) and poly(methacrylic acid) (PMAA), respectively. ^{b)}Molar fraction of midblock PMAA. ^{c,d)}Weight-average molecular weight and molecular weight distribution of the triblock copolymer, respectively.

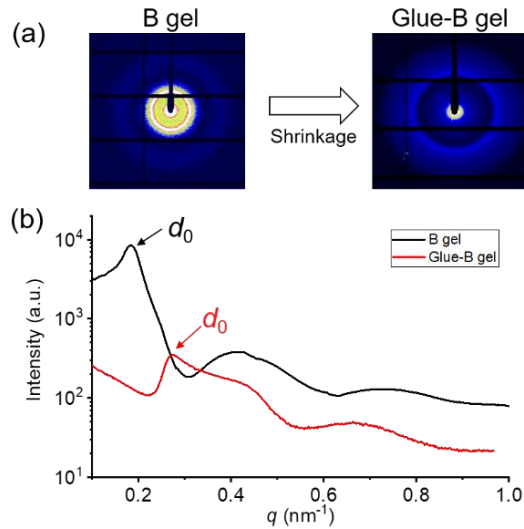


FIG. S1. SAXS results of B and glue-B gels at unstretched state. (a) The 2D SAXS images. (b) 1D scattering intensity profiles. The d_0 , estimated from the peak indicated by the arrow in the figure, is the average distance between neighboring micelles. $d_0 = 34.6$ nm and 22.7 nm for B gel and glue-B gels, respectively. The decrease in d -spacing of glue-B gel is due to the shrinkage of the B gel by hydrogen bond formation, which is confirmed by the good consistency between their d -spacing ratio ($22.7 \text{ nm}/34.6 \text{ nm} = 0.71$) and sample thickness ratio ($1.1 \text{ mm}/1.5 \text{ mm} = 0.72$) of glue-B gel to B gel.

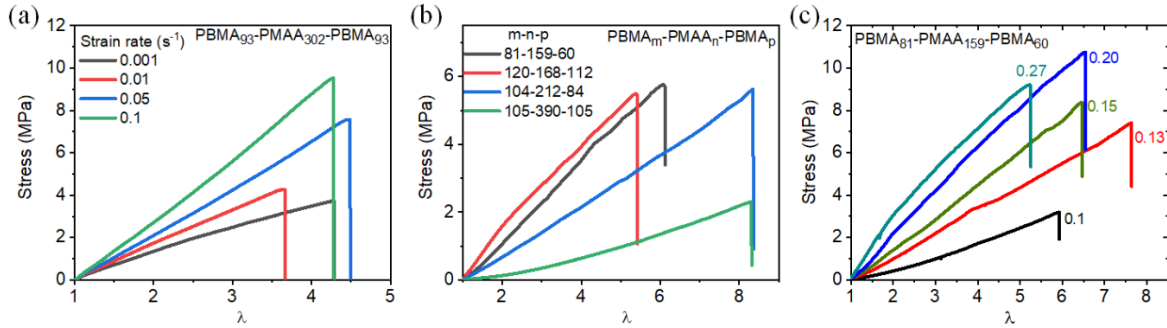


FIG. S2. Nominal stress-stretch curves for glue-B gels in uniaxial tension with (a) different strain rate, (b) chemical structures and (c) triblock copolymer concentrations. The gel preparation method was same as that used in main text. In (a) and (b), the concentrations of the triblock copolymer and AAm monomer were 0.2 wt/wt and 2 mol/L, respectively. In (c), the concentration of AAm monomer was fixed at 2 mol/L, and various concentrations of triblock copolymers were used.

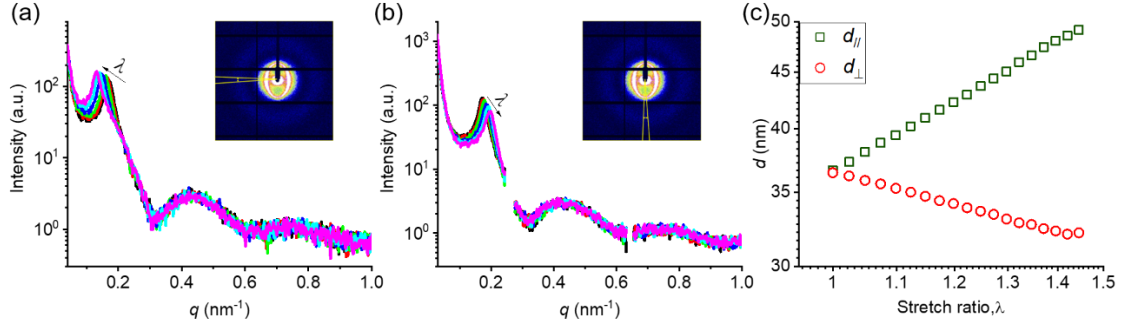


FIG. S3. 1D scattering intensity profiles of B gel stretched at different λ integrated along the direction parallel (a) and perpendicular (b) to the stretching direction. The yellow lines in the 2D SAXS pattern define the horizontal and vertical sector regions for integrating the 1D scattering intensity. (c) The d -spacing change in the direction parallel ($d_{||}$) and perpendicular (d_{\perp}) to the stretching direction during deformation. d spacing stands for the average neighboring inter-micelle distance, which is calculated from $2\pi/q$. The initial strain rate was 0.01 s^{-1} .

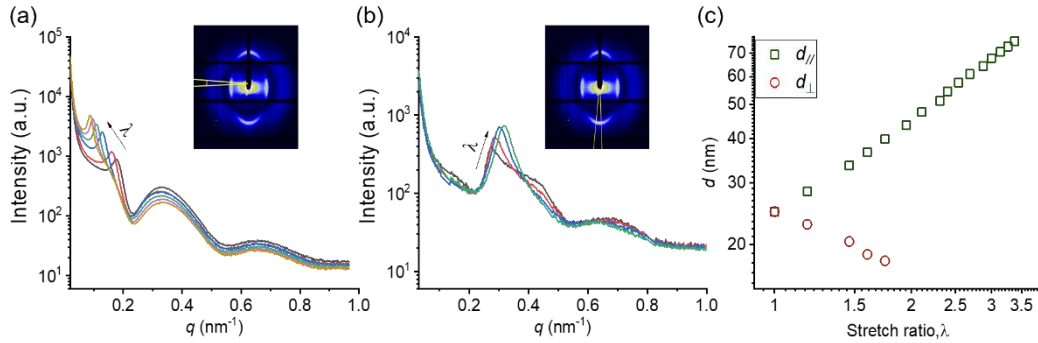


FIG. S4. 1D scattering intensity profiles of glue-B gel stretched at different λ integrated along the direction parallel (a) and perpendicular (b) to the stretching direction. The yellow lines in the 2D SAXS pattern define the horizontal and vertical sector regions for integrating the 1D scattering intensity. (c) The d -spacing change in the direction parallel ($d_{||}$) and vertical (d_{\perp}) to the stretching direction. The initial strain rate was 0.01 s^{-1} .

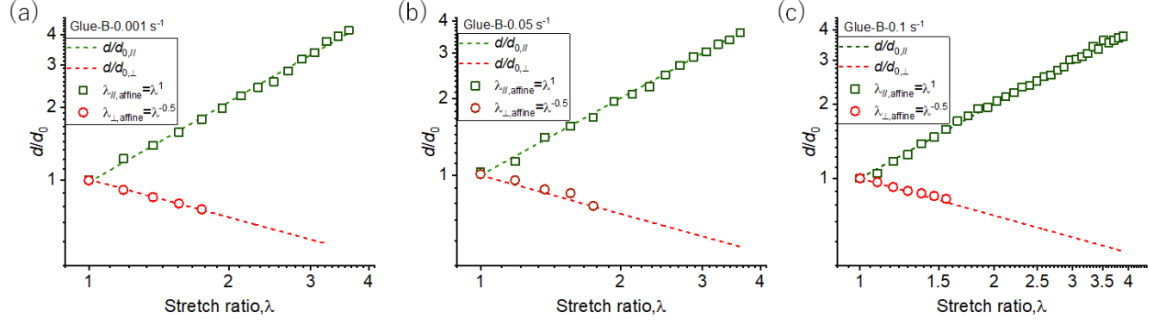


FIG. S5. Microscopic deformation ratio (d/d_0) in the parallel (\parallel) and perpendicular (\perp) directions of stretching versus stretching ratio λ for glue-B gel at initial strain rate of (a) 0.001 s^{-1} , (b) 0.05 s^{-1} and (c) 0.1 s^{-1} . The dotted lines are for affine deformation.

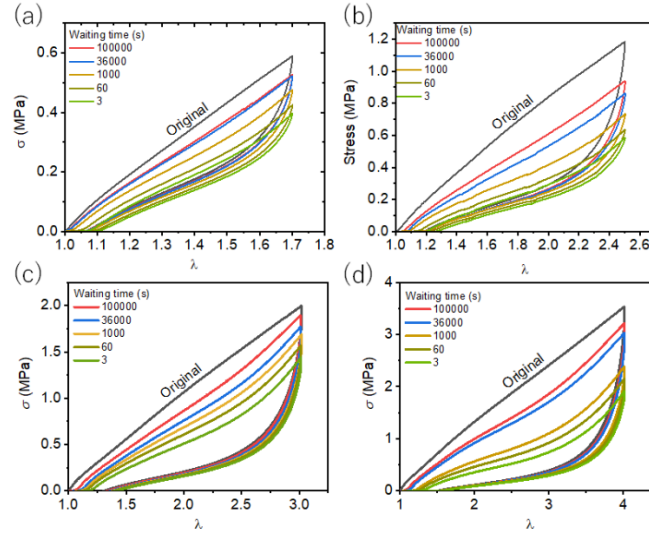


FIG. S6. Loading-unloading curves of the cyclic tensile test of the glue-B gel at different waiting times between the first and second cycles for (a) $\lambda = 1.7$, (b) $\lambda = 2.5$, (c) $\lambda = 3.0$, and (d) $\lambda = 4.0$. The stretching velocity keeps constant as 0.2 mm/s for loading and unloading, and the initial strain rate for loading was 0.01 s^{-1} .

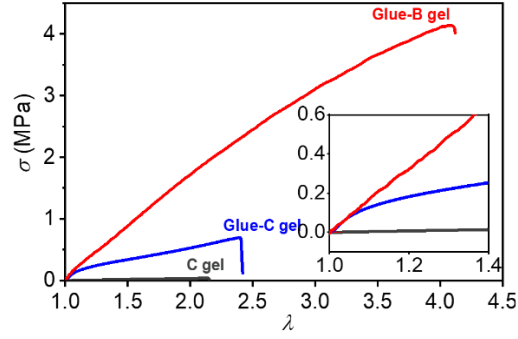


FIG. S7. Mechanical performance comparison between glue-B gel, C gel and glue-C gel in uniaxial tensile test at an initial strain rate 0.01 s^{-1} .

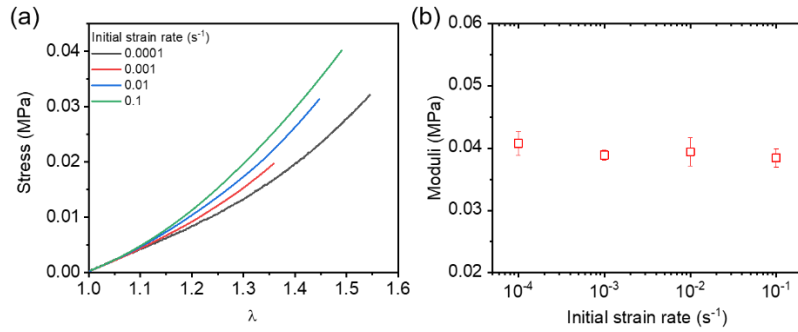


FIG. S8. (a) Nominal stress-elongation curves of the B gel under different initial strain rates ranging from 0.0001 to 0.1 s^{-1} . (b) The moduli of B gel as a function of initial strain rate.

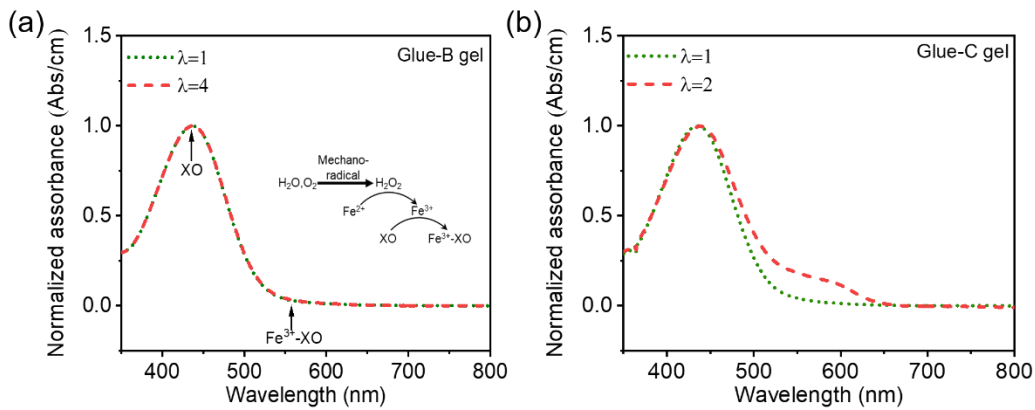


FIG. S9. Comparison of mechanochemical color change between glue-B and glue-C gels based on Fenton reaction. The UV-visible spectra of (a) glue-B gel and (b) glue-C gel fed with $100 \mu\text{M} (\text{NH}_4)_2\text{Fe}^{\text{II}}(\text{SO}_4)_2$, $100 \mu\text{M} \text{ XO}$, and $20 \text{ mM} \text{ H}_2\text{SO}_4$. The peaks at around 440 and 580 nm correspond to unbonded XO and $\text{Fe}^{3+}\text{-XO}$ complexes, respectively.

Reference

1. M. E. Seitz, W. R. Burghardt, K. T. Faber, K. R. Shull, Self-assembly and stress relaxation in acrylic triblock copolymer gels. *Macromolecules* **40**, 1218–1226 (2007).
2. Y. N. Ye, *et al.*, Relaxation Dynamics and Underlying Mechanism of a Thermally Reversible Gel from Symmetric Triblock Copolymer. *Macromolecules* **52**, 8651–8661 (2019).
3. T. L. Chantawansri, T. W. Sirk, Y. R. Sliozberg, Entangled triblock copolymer gel: Morphological and mechanical properties. *J. Chem. Phys.* **138**, 24908 (2013).
4. C. Ortiz, G. Hadziioannou, Entropic elasticity of single polymer chains of poly (methacrylic acid) measured by atomic force microscopy. *Macromolecules* **32**, 780–787 (1999).
5. M. E. Seitz, W. R. Burghardt, K. R. Shull, Micelle morphology and mechanical response of triblock gels. *Macromolecules* **42**, 9133–9140 (2009).
6. T. Matsuda, R. Kawakami, R. Namba, T. Nakajima, J. P. Gong, Mechanoresponsive self-growing hydrogels inspired by muscle training. *Science (80-.).* **363**, 504–508 (2019).
7. M. Sambasivam, A. Klein, L. H. Sperling, Energy-consuming micromechanisms in the fracture of glassy polymers. 2. Effect of molecular weight on the fracture of polystyrene. *Macromolecules* **28**, 152–159 (1995).
8. E. Ducrot, Y. Chen, M. Bulters, R. P. Sijbesma, C. Creton, Toughening elastomers with sacrificial bonds and watching them break. *Science (80-.).* **344**, 186–189 (2014).